Biochimica et Biophysica Acta, 979 (1989) 193–207
Elsevier

BBA 74334

Inhibition of inorganic anion transport across the human red blood cell membrane by chloride-dependent association of dipyridamole with a stilbene disulfonate binding site on the band 3 protein

Barbara Legrum and Hermann Passow

Max-Planck-Institut für Biophysik, Frankfurt am Main (F.R.G.)

(Received 27 September 1988)

Key words: Anion transport; Erythrocyte; Dipyridamole; Band 3 protein

The inhibition of inorganic anion transport by dipyridamole (2,6-bis(diethanolamino)-4,8-dipiperidinopyrimido[5,4-*d*]pyrimidine) takes place only in the presence of Cl^-, other halides, nitrate or bicarbonate. At any given dipyridamole concentration, the anion flux relative to the flux in the absence of dipyridamole follows the equation: $J_{rel} = (1 + \alpha_2[Cl^-])/(1 + \alpha_4[Cl^-])$ where α_2 and α_4 are independent of $[Cl^-]$ but dependent on dipyridamole concentration. At high $[Cl^-]$ the flux approaches α_2/α_4, which decreases with increasing dipyridamole concentration. Even when both $[Cl^-]$ and dipyridamole concentration assume large values, a small residual flux remains. The equation can be deduced on the assumption that Cl^- binding allosterically increases the affinity for dipyridamole binding to band 3 and that the bound dipyridamole produces a non-competitive inhibition of sulfate transport. The mass-law constants for the binding of Cl^- and dipyridamole to their respective-binding sites are about 24 mM and 1.5 μM, respectively (pH 6.9, 26 °C). Dipyridamole binding leads to a displacement of 4,4′-dibenzoylstilbene-2,2′-disulfonate (DBDS) from the stilbenedisulfonate binding site of band 3. The effect can be predicted quantitatively on the assumption that the Cl^--promoted dipyridamole binding leads to a competitive replacement of the stilbenedisulfonates. For the calculations, the same mass-law constants for binding of Cl^- and dipyridamole can be used that were derived from the kinetic studies on Cl^--promoted anion transport inhibition. The newly described Cl^- binding site is highly selective with respect to Cl^- and other monovalent anion species. There is little competition with SO_4^{2-}, indicating that Cl^- binding involves other than purely electrostatic forces. The affinity of the binding site to Cl^- does not change over the pH range 6.0–7.5. Dipyridamole binds only in its deprotonated state. Binding of the deprotonated dipyridamole is pH-independent over the same range as Cl^- binding.

Introduction

Dipyridamole (also called persantine, 2,6-bis(diethanolamino)-4,8-dipiperidinopyrimido[5,4-*d*]pyrimidine) is a drug that potentiates vasodilatation (including coronary dilatation) by adenosine and adenine nucleotides, blocks platelet aggregation by adenosine diphosphate, and inhibits phosphodiesterase activity, thereby promoting an accumulation of cAMP. The potentiation of nucleoside action on the circulation is probably the indirect consequence of an inhibition of adenosine uptake from the blood plasma by the red cells (for a summary of the pharmacological actions, see Ref. 1). In addition to adenosine transport, dipyridamole also inhibits other transport processes, including the band 3 protein-mediated anion exchange across the red cell membrane [2]. In red cells suspended in media containing chloride as the predominant anion species, the inhibition of both chloride and sulfate transport is about equal. At 8 °C the $K_{1/2}$ for dipyridamole is about 5 μM and hence similar to the value pertaining to such powerful anion transport inhibitors as the stilbenedisulfonate 4,4′-dinitrostilbene-2,2′-disulfonate (DNDS, Ref. 3).

In the present paper we report that in the absence of Cl^- dipyridamole produces little if any inhibition of

Abbreviations: H_2DIDS, 4,4′-diisothiocyanodihydrostilbene-2,2′-disulfonate; DBDS, 4,4′-dibenzoylstilbene-2,2′-disulfonate; DNDS, 4,4′-dinitrostilbene-2,2′-disulfonate; N_2ph-F, 2,4-dinitrofluorobenzene.

Correspondence: H. Passow, Max-Planck-Institut für Biophysik, Frankfurt am Main, Heinrich-Hoffmann-Strasse 7, 6000 Frankfurt am Main 71, F.R.G.

0005-2736/89/$03.50 © 1989 Elsevier Science Publishers B.V. (Biomedical Division)

sulfate or phosphate transport. Addition of chloride promotes the inhibition of both transport processes by the agent. A more detailed investigation of the effects of increasing [Cl^-] on sulfate transport showed that $K_{1/2}$ decreases until a limiting value of about 1.5 μM is reached. These results prompted us to perform a more extensive study on the combined effects of dipyridamole and chloride on sulfate transport and to attempt an interpretation of the data in terms of chloride-dependent dipyridamole binding to a site that is allosterically linked to the substrate binding site. The chloride-dependent dipyridamole binding takes place at a stilbenedisulfonate binding site or a site allosterically linked to the latter.

After the completion of our experimental work and while we were engaged in its theoretical analysis, we became aware that Schnell and associates submitted for publication some preliminary experimental results on the same subject. Their paper includes no data on dipyridamole binding and no attempt was made to provide a quantitative interpretation. The emphasis of the present study is on the demonstration of a relationship between dipyridamole binding to the band 3 protein and the inhibition of anion transport and on the quantitative description of that relationship.

Materials and Methods

Human Rh^+ blood was obtained from the blood bank and used within 3 to 5 days after withdrawal.

The experiments were performed with intact red cells or resealed red cell ghosts. In the intact red cells the intracellular concentrations were adjusted by washing in media of the appropriate composition in the presence of Nystatin as described by Cass and Dalmark [4]. In the ghosts, adjustment was achieved by resealing in the desired media as described by Schwoch and Passow [5]. In all experiments, the concentrations inside and outside the red cells or ghosts were identical.

Dinitrophenylation and treatment with $^3H_2$DIDS of red blood cells or ghosts, the isolation of the treated membranes, SDS-polyacrylamide gel electrophoresis and subsequent determination of the radioactivity in the gel slices was performed as described previously [6].

Sulfate equilibrium exchange was measured as in previous work from this laboratory [6]. Dipyridamole was added as an ethanolic solution, giving final ethanol concentrations of 1% (v/v) or less in dipyridamole-containing media. Dipyridamole-free controls always contained corresponding concentrations of ethanol.

Binding of DBDS (4,4'-dibenzoylstilbene-2,2'-disulfonate) to the red cell membrane is associated with a large increment of DBDS fluorescence. This is almost entirely related to DBDS binding to band 3 [7]. In our experiments we determined DBDS binding to band 3 in resealed white ghosts prepared by the column method of Wood and Passow [8]. To eliminate small contributions of DBDS binding to proteins other than band 3 we determined the fluorescence changes brought about by the addition of a band 3 protein-saturating concentration of H_2DIDS (final concentration 20 μM).

When measuring DBDS fluorescence in the presence of dipyridamole, it is necessary to consider the influence of dipyridamole fluorescence. Dipyridamole shows little if any change of fluorescence upon binding to the red cell membrane. Consequently, dipyridamole binding cannot be measured directly by fluorescence determinations. However, it is possible to observe the effect of dipyridamole on DBDS binding and thus to deduce information on dipyridamole binding from dipyridamole/DBDS competition. The emission spectra of dipyridamole and DBDS as produced by excitation at 330 nm partially overlap. At 430 nm the emission spectrum of dipyridamole reaches a minimum while the DBDS emission is only 5% less than at its maximum at 420 nm. Hence all our measurements were executed at the former wavelength. Some of the fluorescence emitted by DBDS is obsorbed by dipyridamole. Under our experimental conditions, absorption is 10% or less. Measuring DBDS fluorescence at 430 nm has the added advantage that under our experimental conditions (using a Zeiss PM Q II photometer and a ghost density of about 2%) the effect of light scattering is negligible. The correction for the effects of the absorption of the exciting light by the contents of the cuvette ('inner filter effect') was performed according to standard procedures.

Variations of dipyridamole fluorescence with hydrogen ion concentration can be described by the mass-law equation: $[H^+] \cdot [\text{dipyridamole}]/[\text{H-dipyridamole}^+] = 5.62 \cdot 10^{-7}$ M, corresponding to a pK value of 6.25. This value was found to be independent of the presence of Cl^-, SO_4^{2-} and DBDS at the concentrations used in our work, indicating that none of these ions combine with the inhibitor.

Isolation of red cell membranes and their SDS-polyacrylamide gel electrophoresis was performed as described previously [6].

All chemicals were analytical grade. The dipyridamole originated from Prof. B. Deuticke, Rheinisch-Westfälische Technische Hochschule, Aachen. We are indebted to Prof. H. Fasold for the synthesis of DBDS.

Results

(1) Effects of chloride on inhibition of sulfate transport by dipyridamole

Using the Nystatin technique of Cass and Dalmark [4], human red cells were equilibrated in media containing either 15 or 150 mmol/l SO_4^{2-} as the only penetrating anion species. After addition of dipyridamole at concentrations up to 32 μmol/l, sulfate equilibrium exchange was measured. Fig. 1 shows that there is only

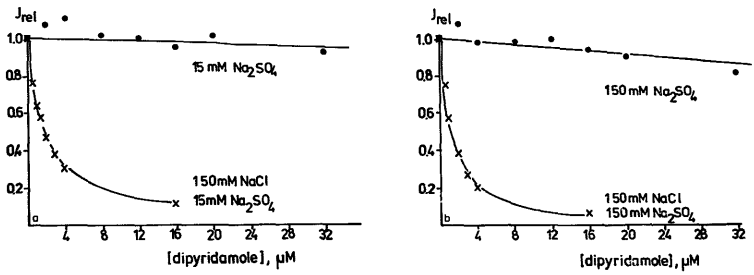

Fig. 1. Effect of chloride on inhibition of sulfate equilibrium exchange by dipyridamole. Intact red cells, pH 6.9, 25.5 °C. The curves pertaining the the data points observed in the presence of chloride (150 mM) were calcualted using a non-linear curve fitting procedure to fit the data to the equation $J_p/J_{p=0} = 1/(K_{1/2} + p) + \text{constant}$, where $J_p/J_{p=0}$ represents the sulfate flux at dipyridamole concentration p as a fraction of sulfate flux at $p = 0$. Left-hand and right-hand panel: experiments performed in the presence of 15 and 150 mM Na_2SO_4, respectively. The $K_{1/2}$ values were 1.9 and 1.3 µM, respectively. Ordinate: $J_{rel} = J_p/J_{p=0}$, abscissa: dipyridamole concentration.

very little inhibition which is possibly related to the presence of traces of bicarbonate in the cell suspension (see below). When the red cells are equilibrated by the same method with 15 or 150 mmol/l Na_2SO_4 in the presence of a fixed concentration of 150 mmol/l NaCl or KCl, dipyridamole produces a strong inhibition with half-inhibition constants of 1.28 and 1.95 µM, respectively.

The effects of chloride were studied in more detail by varying (1) the dipyridamole concentration at a range of fixed chloride concentrations (Table I), and (2) the chloride concentration at a range of fixed dipyridamole concentrations (Fig. 2).

TABLE I

Inhibition of sulfate equilibrium exchange by dipyridamole: Dependence of half-inhibition constant ($K_{1/2}$) on chloride concentration

Sulfate equilibrium exchange was measured at a range of fixed chloride concentrations as a function of dipyridamole concentration. The empirical $K_{1/2}$ values were obtained by non-linear least-squares curve fitting to the equation: $J_{rel} = 1/(K_{1/2} + p) + \text{constant}$ where the constant represents the residual flux at maximal inhibition (average: 5.8% of flux without inhibitor). The predictions are based on the equation $K_{1/2} = K_8 \cdot (a + K_1)/a$ where $K_8 = 1.47$ µM and $K_1 = 24.2$ mM (averages from Table VI). a represents the chloride concentration. The cosntants K_1 and K_8 are defined in Appendix A, where the equation is derived (Eqn. A-5). n.d., not determined.

$[Cl^-]$ (mM)	$K_{1/2}$ (µM), as measured in the presence of:		Predicted (model II)
	150 mM SO_4^{2-}	15 mM SO_4^{2-}	
3.75	16.0	n.d.	11.0
7.50	7.6	6.4	6.2
15.0	3.7	n.d.	3.8
40.0	2.0	2.6	2.4
150.0	1.3	1.9	1.7

The first set of these experiments followed the same pattern as the experiments presented in Fig. 1. The $K_{1/2}$ values listed in the table decrease with increasing $[Cl^-]$ and tend to approach a limiting value for high Cl^- concentrations somewhere between $K_{1/2} = 1$ µM and 2 µM.

When the chloride concentration was raised at fixed concentrations of dipyridamole the sulfate fluxes decreased and also approached limiting values. These values were a function of the dipyridamole concentration. Even at very high concentrations of both dipyridamole and chloride a small residual flux remained. The results

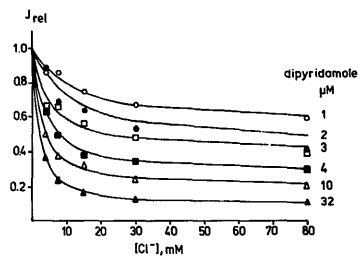

Fig. 2. Sulfate equilibrium exchange measured at fixed concentrations of both SO_4^{2-} (15 mM) and dipyridamole as a function of $[Cl^-]$. Red cell ghosts. pH 6.9, 26 °C. Ordinate: SO_4^{2-} flux at the chloride concentrations indicated on the abscissa and the dipyridamole concentrations indicated on the curves relative to the flux in the absence of dipyridamole. The drawn curves were obtained by non-linear least-squares computer fits to the equation $J_{rel} = (1 + \alpha_2 a)/(1 + \alpha_4 a)$ where α_2 and α_4 represent constants and a indicates the concentration of $[Cl^-]$. The α values are listed in Table II.

of these measurements can be represented by the equation

$$J_{rel} = (1 + \alpha_2 a)/(1 + \alpha_4 a) \quad (1)$$

where J_{rel} is the flux at dipyridamole concentration p relative to the flux at $p = 0$ as measured at the Cl^- concentration a. α_2 and α_4 are constants that vary with the dipyridamole concentration and depend on the residual flux that persists when a and p tend to large values (see below). At larger values of a J_{rel} approaches α_2/α_4, i.e. the ratio of the two constants yields the asymptotic value of the relative flux at high chloride concentration.

In Table II the values for α_2, α_4 and the ratio α_2/α_4 are listed as calculated by means of a non-linear least-squares computer fit to the data in Fig. 2. In addition, the table contains values of α_2 and α_4 for essentially similar experiments which were performed at fixed sulfate concentrations of 150 mM and 300 mM instead of 15 mM as in the experiments depicted in Fig. 2. The asymptotic values α_2/α_4 tend to be somewhat higher at 150 and 300 mM SO_4^{2-} than at 1 mM SO_4^{2-}. However, the scatter of the data is large and hence this tendency is not well established. It should be noted that the relative fluxes measured at 80 mM $[Cl^-]$ are still somewhat larger than the asymptotical values α_2/α_4. In Fig. 3 the relative sulfate fluxes measured at $[Cl^-] = 80$ mM are compared to the fluxes calculated for that Cl^- concentration by means of Eqn. 1 using the α's in Table II. The data points scatter now near the identity line, indicating that the deviations from the asymptotic values seen in Table II seem to be significant.

TABLE II

Effect of Cl^- on the inhibition of SO_4^{2-} equilibrium exchange by dipyridamole

The numerical values of α_2 and α_4 were obtained by non-linear least-squares computer fits of experimental data to the equation: $J_{rel} = (1 + \alpha_2 \cdot a)/(1 + \alpha_4 \cdot a)$ (Appendix A, Eqn. A-3). a represents the Cl^- concentration in cells and medium, J_{rel} the sulfate flux at dipyridamole concentration p divided by the corresponding flux at $p = 0$. The data listed for $[SO_4^{2-}] = 15$ mM are derived from the curves in Fig. 2, the others from similar experiments at SO_4^{2-} concentrations of 150 and 300 mM. The ratio α_2/α_4 indicates the asymptotic values of J_{rel} at high chloride concentrations. It is compared with the ratios measured at $[Cl^-] = 80$ mM. These measured ratios are plotted in Fig. 3 against the ratios calculated for $[Cl^-] = 80$ mM.

p (μM)	α_2	α_4	α_2/α_4	J_{rel} ($a = 80$ mM)	$[SO_4^{2-}]$ (mM)
1	0.0419	0.0785	0.534	0.595	15
2	0.0378	0.0905	0.418	0.410	
3	0.0901	0.228	0.395	0.392	
4	0.0774	0.288	0.268	0.305	
10	0.0851	0.441	0.193	0.209	
32	0.0571	0.624	0.083	0.108	
1	0.0193	0.0416	0.465	0.588	150
2	0.0495	0.134	0.369	0.420	
3	0.0665	0.177	0.376	0.380	
4	0.0436	0.152	0.288	0.325	
5	0.0587	0.194	0.302	0.408	
10	0.138	0.538	0.256	0.288	
32	0.186	1.07	0.174	0.262	
1	0.0277	0.0442	0.627	0.728	300
2	0.0465	0.0982	0.474	0.540	
3	0.1072	0.2058	0.521	0.566	
4	0.0391	0.124	0.317	0.372	
5	0.0845	0.166	0.509	0.543	
10	0.0720	0.343	0.209	0.237	
32	0.0819	0.493	0.166	(0.316)	

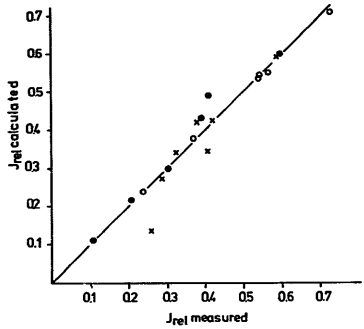

Fig. 3. Plot of sulfate flux J_{rel} measured at $[Cl^-] = 80$ mM against the flux calculated for this Cl^- concentration from the equation $J_{rel} = (1 + \alpha_2 a)/(1 + \alpha_4 a)$. The α values were taken from Table II. The symbols ●, ×, ○ refer to 15, 150, 300 mM $[SO_4^{2-}]$, respectively. At each sulfate concentration, flux measurements were performed at the dipyridamole concentrations (μM): 1, 2, 3, 4, 10, 32 and at 150 and 300 mM SO_4^{2-} also at 5 μM dipyridamole. The straight line represents identity.

In the experiment represented in Fig. 4, the effect of chloride concentration on the inhibition by a fixed concentration of 2 μM dipyridamole was studied at a fixed ratio between $[Cl^-]$ and $[SO_4^{2-}]$ of 1:10. The effect observed can be represented by Eqn. 1, using the average of the α_2 and α_4 values listed in Table II for the dipyridamole concentration of 2 μM and pertaining to the three sulfate concentrations used. Thus the chloride-promoted inhibition of sulfate transport by dipyridamole is only little affected by increasing the SO_4^{2-} concentration from 15 to 300 mM. Nevertheless, a replot of the fluxes measured at the sulfate concentrations of 15, 150 and 300 mM (Table II) reveals that at each chloride concentration used a slight increase of sulfate flux occurs (Fig. 5). It is unlikely, however, that this is the consequence of a replacement of Cl^- from its

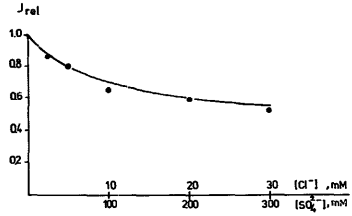

Fig. 4. Effect of dipyridamole (2 μM) on SO_4^{2-} equilibrium exchange as a function of Cl^- concentration. The ratio $[Cl^-]/[SO_4^{2-}]$ was maintained at 1:10. The drawn curve was calculated by means of Eqn. 1 using the averages of the values for α_1 and α_2 observed at 15, 150 and 300 mM Na_2SO_4 (Table II). ($\alpha_2 = 0.0466 \pm 0.006$, $\alpha_4 = 0.108 \pm 0.023$). This corresponds to $K_1 = 25.6$ mM, $K_8 = 1.13$ μM and $q_K = 0.08$. Ordinate: sulfate flux at the Cl^- and SO_4^{2-} concentrations indicated on the abscissa divided by the corresponding fluxes as measured in the absence of dipyridamole (J_{rel}).

TABLE III

Promotion of the effects of persantine on sulfate equilibrium exchange by various monovalent anions species

In all experiments, the concentrations of SO_4^{2-} and dipyridamole were 150 mM and 15 μM, respectively. The concentration of the monovalent anions was 7.5 mM. The pH was 6.9, except in the experiments with HCO_3^- were the pH was 7.2. J_{rel} = flux in presence of dipyridamole relative to flux in absence of dipyridamole. Each data point represents the average of two separate experiments which agreed to within less than 10%.

Monovalent anion species	J_{rel} (%)
None	103
F^-	88
Cl^-	40
Br^-	42
I^-	74
HCO_3^-	62
NO_3^-	40 [a]

[a] In 160 mM $NaNO_3$, pH 6.9, 26 °C, $K_{1/2}$ is 4.5 μM. The residual flux at maximal inhibition is 10%.

specific binding site, since the effect is independent of the Cl^- concentration in the medium. Possibly it simply represents an effect of increasing ionic strength.

The pH dependence of the effect observed in the joint presence of Cl^- and dipyridamole was studied only at fixed concentrations of sulfate (1 mM) and chloride (30 mM) at three different dipyridamole concentrations. The relative flux decreases when the pH is increased from 6.0 to 7.5 and then approaches a plateau or a flat minimum which extends at least up to pH 7.7 (Fig. 6). The effect can be almost completely accounted for by a change of protonation of dipyridamole, assum-

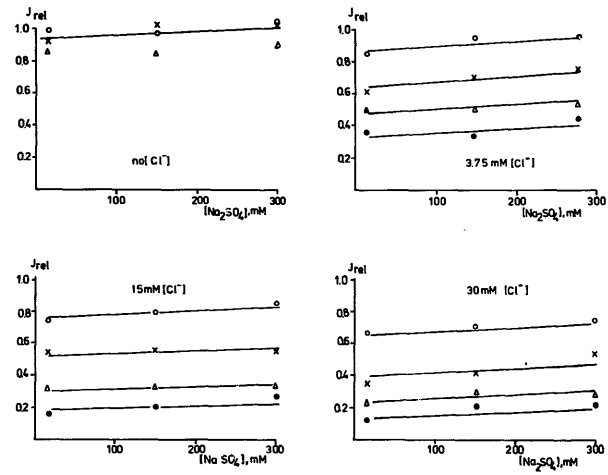

Fig. 5. Effect of varying $[SO_4^{2-}]$ on the action of dipyridamole on sulfate equilibrium exchange. Ordinate: J_{rel}. Abscissa: $[SO_4^{2-}]$, mM. The dipyridamole concentrations (in μM) are: ○, 1; ×, 4; △, 10; ●, 32.

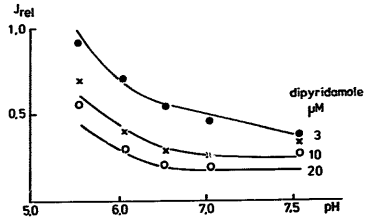

Fig. 6. pH-dependence of the effects of dipyridamole at a Cl^- concentration of 30 mM and a SO_4^{2-} concentration of 150 mM. Red cell ghosts. Ordinate: sulfate flux J_{rel}. Abscissa: pH. The drawn lines were calcualted on the assumption that the pH dependence is exclusively related to the protonation of dipyridamole (see Discussion for details).

ing that only the deprotonated form produces inhibition (see Discussion).

(2) Effects of other monovalent anions on inhibition of sulfate transport by dipyridamole

The inhibition by dipyridamole is not only promoted by chloride but also by other monovalent anion species (Table III). The inhibitory potencies of these other anion species were studied by measuring the inhibition produced by 15 μmol/l dipyridamole in the presence of 7.5 mmol/l of the various anion species. The sequence $NO_3^- = Cl^- = Br^- > I^- > F^-$ was observed. HCO_3^- was also effective. However, the result depicted in the table is not strictly comparable with the others since it was obtained at pH 7.2 rather than 6.9 as in the experiments with the halides.

(3) Phosphate transport and dipyridamole

Experiments with phosphate deserve a special interest. At pH 6.9 about 50% of this anion exists in the divalent form HPO_4^{2-} and the remaining 50% in the monovalent form $H_2PO_4^-$. It is believed that the penetration takes place predominantly in the monovalent form (reviewed in Ref. 9).

The presence of phosphate at pH 6.9 does not promote the inhibition by dipyridamole of the penetration of the sulfate (not shown). Moreover, phosphate transport is also not inhibited by dipyridamole, as long as no Cl^- is present. Upon addition of Cl^-, phosphate transport is inhibited, in a manner similar to that described for sulfate transport (Table IV).

(4) Inhibition of chloride transport

Table V indicates that the inhibition of chloride transport by dipyridamole is also promoted by chloride. Thus it is clear that the Cl^--dependent dipyridamole

TABLE IV

Effect of Cl^- on the inhibition of phosphate transport by dipyridamole

15 mM sodium phosphate with and without 130 mM NaCl, pH 6.9, 26°C.

Dipyridamole (μM)	Cl^-	J_{rel}
0	0	1.00
4	0	0.91
8	0	0.89
32	0	0.85
0	130	1.00
4	130	0.37
8	130	0.33
32	130	0.30

binding leads to a generalized inhibition of both monovalent and divalent anion transport.

(5) Chloride-promoted effects of dipyridamole on DBDS binding

The experiments described below indicate that dipyridamole interferes with the binding of the stilbenedisulfonate DBDS to the band 3 protein and that this interference is promoted by the presence of chloride.

In aqueous solution, DBDS is slightly fluorescent. Upon binding to band 3 the fluorescence is greatly enhanced. This enhancement can be used for quantitative investigations of DBDS binding (see Methods).

Figs. 7a and 7b show that DBDS binding follows a simple saturation curve. The half saturation constant $K_{1/2}$ depends slightly on the ionic composition of the medium. From the data shown in these figures and from additional measurements (not shown), we obtained numerical values for $K_{1/2}$. In the absence of penetrating anion species, $K_{1/2}$ is 0.68 μM; in the presence of 130 mM Cl^-, 1.1 μM; and in the presence 108 mM SO_4^{2-}, 0.5 μM.

When DBDS binding is measured in the presence of dipyridamole, $K_{1/2}$ remains unaffected provided the measurements are performed in a medium containing 108 mM SO_4^{2-}. If the medium contains instead 130 mM NaCl, $K_{1/2}$ for DBDS binding increases to 26.8 μM suggesting that dipyridamole is capable of competing

TABLE V

Effect of dipyridamole (32 μM) on Cl^- equilibrium exchange

0°C, pH 7.4, EDTA buffer, 20 mM. Red cell ghosts.

[NaCl] (mM)	Inhibition (%)
7.5	46.7
7.5	41.2
130	71.9
130	65.7

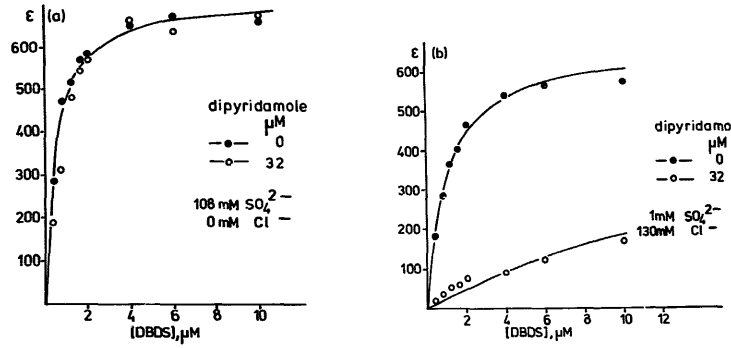

Fig. 7. DBDS-binding to resealed white ghosts (see Methods) as determined by measuring fluroescence enhancement at 430 nm (see Methods). The measurements were made either in the absence or in the presence of 32 μM dipyridamole. (a) Measurements in chloride-free sulfate medium: $K_{1/2}$ = 0.5 μM. (b) Measurements in presence of 130 mM Cl^-: $K_{1/2}$ without dipyridamole 1.1 μM, with dipyridamole 26.8 μM.

with DBDS for a common binding site or combines with a site that is allosterically linked to the stilbenedisulfonate binding site.

The effect of systematically increasing Cl^- concentration at a fixed dipyridamole concentration on the release of DBDS from band 3 is shown in Fig. 8. The relationship observed resembles that described for the effect of chloride on inhibition by dipyridamole of

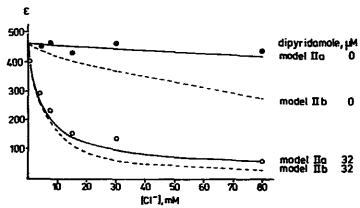

Fig. 8. Effect of Cl^- concentration on replacement of DBDS from band 3 by dipyridamole. Ordinate: DBDS binding as determined by measuring H_2DIDS-sensitive fluorescence enhancement of DBDS at 430 nm. ●, Control without dipyridamole. ○, 32 μM dipyridamole present. The drawn lines were calcualted by means of Eqn. B-1, the dashed lines by means of Eqn. B-2, using the values for chloride and dipyridamole binding (K_1 and K_8, respectively) in Table VI and the values for the mass-law constants of DBDS binding in the absence of dipyridamole (K_{14}, K_{16}, K_{101}) indicated in the text. Eqn. B-1 refers to competition between dipyridamole and DBDS for the dipyridamole-binding modifier site, Eqn. B-2 to allosteric effects of dipyridamole-binding to the dipyridamole-binding modifier site on competition between Cl^- and DBDS at the Cl^- binding modifier site.

anion transport (Fig. 2). It seems most plausible to assume, therefore, that the effects of dipyridamole on both anion transport and stilbene binding are due to dipyridamole binding to the same site and that this site is identical to or allosterically linked with the stilbene disulfonate binding site on band 3.

(6) Localization of the site of action of dipyridamole

In view of the findings described above, it seemed useful to explore further the interaction of dipyridamole with the stilbenedisulfonate binding site. In order to do this, we made use of the previous observation that a specific lysine residue called Lys *a* provides one of the amino groups involved in the covalent binding of the isothiocyanate residues of stilbenedisulfonates like H_2DIDS or SITS [6]. Lys *a* has an abnormally low p*K* value and reacts easily with 2,4-dinitrofluorobenzene (N_2ph-F). The rate of reaction of this residue is reduced by the presence of noncovalently binding stilbene disulfonates such as DNDS. The rate of dinitrophenylation of Lys *a* is also reduced when the reaction with N_2ph-F takes place in the presence of dipyridamole. This effect is only seen when the reaction is performed in the presence of Cl^- as the principal anions species. In the absence of Cl^-, in an all SO_4^{2-} medium, dipyridamole leaves the rate of dinitrophenylation unaltered. Thus, the effect of dipyridamole on the susceptibility of Lys *a* to react with N_2ph-F depends on the nature of the substrate anion, similar to the effect of dipyridamole on band 3-mediated anion transport. It is most likely, therefore, that the mode of action of dipyridamole on anion transport involves binding to or allosterical mod-

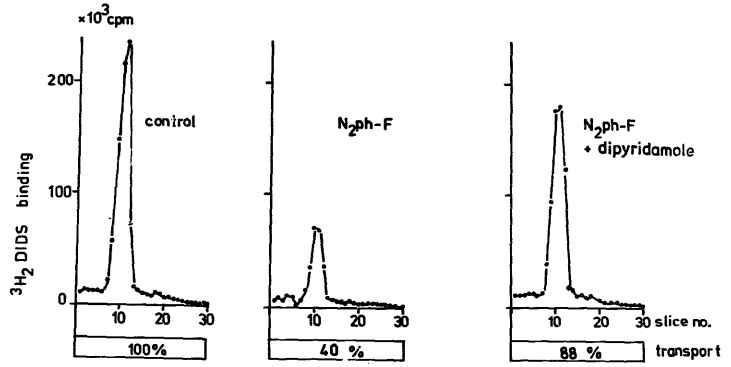

Fig. 9. Effect of dipyridamole on the dinitrophenylation of Lys a on the band 3 protein in chloride medium (130 mM NaCl, 20 mM EDTA, pH 7.4). The effect of the N_2ph-F treatment was determined by (i) flux measurements ('transport', expressed in the figure as a percentage of the flux in the untreated control) and by (ii) determination of the unmodified Lys a on band 3 by 'titration' with $^3H_2$DIDS. The SDS-polyacrylamide gel electropheretogram designated 'control' shows the H_2DIDS binding capacity of Lys a in untreated ghosts. This capacity is reduced when ghosts had been treated with N_2ph-F (125 μM, pH 7.4, 37°C, 30 min) prior to the exposure to $^3H_2$DIDS. When the N_2ph-F treatment is performed in the presence of dipyridamole (32 μM) the capacity of Lys a to combine with $^3H_2$DIDS is largely preserved. Each data point refers to the radioactivity of $^3H_2$DIDS in a gel slice. The peaks are located at the site of migration of band 3.

ification of the stilbenedisulfonate binding site on band 3.

The experiments on which this conclusion is based are represented in Figs. 9 and 10. Resealed red cell ghosts had first been equilibrated with media containing either Cl^- or SO_4^{2-} as the predominant anion species (called Cl^- or SO_4^{2-} medium, respectively). They were then exposed to N_2ph-F at 37°C. After 30 min the

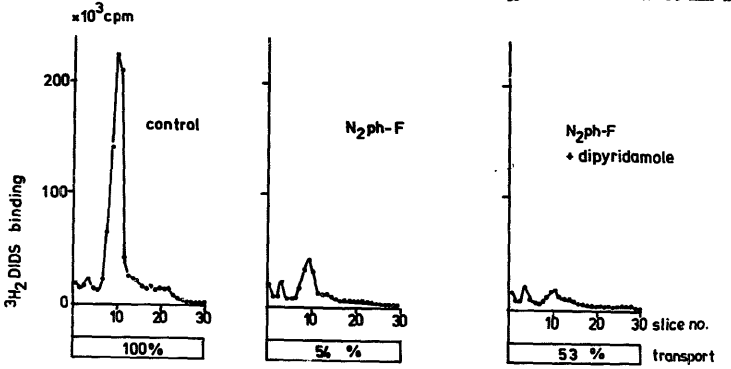

Fig. 10. Effect of dipyridamole on dinitrophenylation of Lys a on the band 3 protein in sulfate medium (108 mM Na_2SO_4, 20 mM EDTA, pH 7.4, no Cl^- present). Same experimental arrangement as in Fig. 9. The figure shows that in sulfate medium the presence of dipyridamole during exposure to N_2ph-F (125 μM, pH 7.4, 37°C, 30 min) can neither prevent the inhibition of sulfate equilibrium exchange ('transport') nor the dinitrophenylation of Lys a and the consequent decrease of the capacity of Lys a to bind $^3H_2$DIDS covalently.

reaction was interrupted by washing the ghosts in N_2ph-F-free medium. Each batch of cells was then subdivided into two. One of them was used for flux measurements. The other was used to determine the number of modified band 3 molecules per cell by titration with $^3H_2$DIDS. This titration is based on the fact that the lysine residues which had been dinitrophenylated are no longer capable of covalent reaction with $^3H_2$DIDS. Hence, the decrease of the capacity of band 3 for covalent $^3H_2$DIDS binding is a measure of the number of Lys *a* residues modified during the treatment with N_2ph-F. Our findings show that the capacity of the red cell ghosts to combine with $^3H_2$DIDS decreases upon dinitrophenylation. When the exposure to N_2ph-F takes place in the presence of dipyridamole, this decrease is largely prevented, provided the exposure takes place in Cl^- medium (Fig. 9). If, however, the exposure is performed in SO_4^{2-} medium, dipyridamole is ineffective (Fig. 10).

Discussion

(1) The specificity and function of the chloride binding modifier site involved in the promotion of dipyridamole binding

Our data show that chloride-promoted binding of dipyridamole to the stilbenedisulfonate binding site of the band 3 protein is responsible for the inhibition of anion transport by dipyridamole. The inhibition is not confined to the transport of divalent anion species and the promotion of the effect is not restricted to chloride since other monovalent anion species, halides as well as bicarbonate, can substitute for Cl^-. Nevertheless, the anion binding site involved in the promotion of dipyridamole binding is highly specific with respect to monovalent anions. A large excess of sulfate (up to 300-fold) exerts only little effect on the capacity of Cl^- to promote dipyridamole binding. Thus the forces involved in the binding of Cl^- to the site are unlikely to be exclusively of electrostatic nature since this could not convey such large selectivity. This conclusion is further supported by the observation that the effects produced by monovalent anion species other than Cl^- may be much smaller or, as in the case of $H_2PO_4^-$, may be virtually absent. Perhaps similar as in a carrier peptide, some specifically arranged amino acid residues on band 3 are able to replace the hydration shell of Cl^- and the other inhibition-promoting inorganic anions, but not of sulfate or phosphate.

It is unknown why the presence of a bound chloride ion is required for dipyridamole binding. Dipyridamole combines with band 3 in its deprotonated, uncharged form (see below). Possibly the negative charge of Cl^- helps to open the hydrophobic cleft at the surface of the band 3 molecule which is believed to serve as a receptacle for stilbenedisulfonates. The stilbenedisulfonates could induce the opening on account of their own negative net charge, while the uncharged dipyridamole is unable to achieve this by itself.

(2) Models of the inhibitory mechanism

(a) Description of models I and II. With the information about the nature of the allosterically interacting binding site for Cl^- and dipyridamole in mind it is possible to design models for the quantitative evaluation of our data. Two models were considered in some detail:

Model I is based on the assumption that on each band 3 molecule there exists in addition to a common transfer site for Cl^- and SO_4^{2-} a modifier site which combines only with Cl^- but not with SO_4^{2-}. This model can be represented by

$$M(a) - T(a, b, p)$$

where M indicates the modifier site, T the transfer site, a chloride, b sulfate and p dipyridamole. The brackets enclose the ligands that are able to combine with the respective sites. Dipyridamole binding to T would be facilitated by chloride binding to M and competitively replace a substrate anion from the transfer site.

Model II is based on the assumption that on each band 3 molecule there exist two modifier sites M and P in addition to the transfer site:

$$\begin{matrix} M(a) - T(a, b) \\ \quad\quad P(p) \end{matrix}$$

Here capital P represents the dipyridamole binding modifier site and the little p in the brackets indicates that this site combines with p but neither with a nor b.

Even without quantitative considerations, it is obvious that model I is not suited for the interpretation of our experimental results. According to this model, inhibition at a given chloride concentration should be reduced or even abolished by the addition of a large excess of sulfate (b), which should release the dipyridamole by competition. This is contrary to observation and suggests at the outset that dipyridamole acts as a noncompetitive inhibitor as represented in model II.

With respect to model II, we assume that the translocation of sulfate bound to the transfer site T can only take place when the dipyridamole binding site P is not occupied by dipyridamole p and that the binding of p requires the occupancy of the modifier site M by chloride (a). Occupancy of M with a is assumed to exert no influence on the translocation rate of the substrate loaded transfer site T (b).

(b) Comments on the mathematical formulation of models I and II: Simplifying assumptions. Models with two or three interacting sites for three different ligand species are fairly complex. A detailed quantitative treat-

ment would lead to expressions the significance of which would be difficult to grasp and the evaluation of which would most likely lead to ambiguous results. Hence simplifying assumptions need to be made. These simplifications are introduced at two levels: firstly in the assumptions underlying the derivations and secondly in the final equations derived after preliminary attempts to fit these still complex expressions to the data.

The first set of assumptions consists of the following:

(i) The binding of the ligands to M, P and T takes place much faster than the translocation of the substrate bound to T. Hence it is possible to calculate ligand binding by applying the mass law. Since the amounts of Cl^-, SO_4^{2-} and dipyridamole in the media inside and outside the cell far exceed the amounts of carrier molecules available, ligand consumption can be neglected.

(ii) The rate of translocation of sulfate is proportional to the number of transport protein molecules in which the transfer site is occupied with sulfate (b). However, the rates of transport may be different, depending on whether or not M or P are occupied by their respective ligands.

(iii) Differences of ligand binding to transport molecules with inward-directed and outward-directed transfer site are disregarded. Thus the calculations of ligand binding include the effects of allosteric interactions between the various binding sites but disregard the effects of conformational changes associated with the translocation step.

(c) Kinetics of chloride-promoted dipyridamole inhibition of anion transport. (See Appendix A, model II, for quantitative treatment.)

The result of the derivations consists of the expression:

$$J_{rel} = \frac{1 + \tau_1 \cdot a + \tau_2 \cdot a^2 + \tau_3 \cdot a^3}{1 + \tau_4 \cdot a + \tau_5 \cdot a^2 + \tau_6 \cdot a^3} \tag{2}$$

where J_{rel} represents the sulfate flux at dipyridamole concentration p relative to the flux at the concentration $p = 0$. The constants τ represent expressions which are independent of a, but dependent on b and p and on the dissociation constants for a, b, and p at the various binding sites.

Preliminary attempts to fit the data to this equation showed that a good fit could be obtained if all terms except the linear terms were neglected. This indicates that some of the interactions that according to the model may occur play a negligible role. We assume that the binding of chloride and sulfate to the transfer site remains unaffected by chloride binding to the modifier site M (i.e. $K_2 = K_3$; $K_5 = K_6$). We further stipulate that there is no dipyridamole binding to P when no chloride is bound to M ($K_7 = K_{10} = K_{11} = \infty$) and that the chloride-promoted dipyridamole binding is not affected by chloride or sulfate binding to T ($K_8 = K_9 = K_{12}$). Under these assumptions we arrive at:

$$J_{rel} = \frac{1 + \alpha_2 \cdot a}{1 + \alpha_4 \cdot a} \tag{3}$$

where J_{rel} = flux at dipyridamole concentration p relative to the flux at $p = 0$, and where

$$\alpha_2 = \frac{1}{K_1} \cdot \left(1 + q_K \frac{p}{K_8}\right)$$

$$\alpha_4 = \frac{1}{K_1} \cdot \left(1 + \frac{p}{K_8}\right) \tag{4}$$

p/K_8 represents the fractional occupancy of P with p and q_K the residual relative flux that persists after all sites P are occupied. At $a \to \infty$, J_{rel} approaches asymptotic values which are a function of p:

$$J_{rel}(a = \infty) = \frac{\alpha_2}{\alpha_4} = \frac{1 + q_K \frac{p}{K_8}}{1 + \frac{p}{K_8}} \tag{5}$$

This prediction is in qualitative agreement with the observations represented in Fig. 2. From the values of α_2 and α_4 in Table II on can calculate the numerical values for the constants q_K, K_1 and K_8 listed in Table VI. The table further shows that essentially similar results are obtained when the experiments are performed in the presence of fixed concentrations of 15, 150 and 300 mM sulfate. This demonstrates the virtual

TABLE VI

K_8, K_1 and q_K for different sulfate concentrations

Approximate values of the dissociation constants of dipyridamole (K_8) and chloride (K_1) as defined by model II described in the text and in Appendix A. q_K is a composite quantity which reflects the fractional residual sulfate flux at maximal inhibition (see Appendix A). $[SO_4^{2-}]$ indicates the sulfate concentration in the medium. pH 6.9, 26°C. For the calculations the values for α_2 and α_4 from Table II were inserted into the equations (see Appendix A, Eqn. A-3): $K_8 = p(q_K - \alpha_2/\alpha_4)/(\alpha_2/\alpha_4 - 1)$ and $K_1 = (1 + p/K_8)/\alpha_4 = (1 + q_K \cdot p/K_8)/\alpha_2$. The q_K values were determined by calculating for a range of assumed values of q_K the corresponding values for K_8 and K_1. For the resulting values of K_1 and K_8 standard deviations were calculated. The assumed q_K value that yielded the lowest standard deviation for K_8 and K_1 was chosen and is represented in the table together with the corresponding values of K_8 and K_1.

$[SO_4^{2-}]$ (mM)	K_8 (μM)	K_1 (mM)	q_K	n
15	1.6±0.4	19.2± 8.3	0.0325	6
150	1.1±0.4	28.7±11.3	0.135	7
300	1.7±0.6	24.6± 9.0	0.070	6

independence of chloride binding to the modifier site (K_1) of sulfate concentration *.

The numerical values for K_1 and K_8 can be used to predict the $K_{1/2}$ values for the inhibition by dipyridamole as measured at fixed chloride concentration:

If $q_K \ll 0.5$, one obtains: $K_{1/2} \approx K_8\left(1+\frac{K_1}{a}\right)$

(Appendix A, Eqn. A-5)

In Table I $K_{1/2}$ values obtained at a range of chloride concentrations are compared with the predictions by this equation, using the averages of the respective values for K_8 and K_1 listed in Table VI. The agreement between observation and calculation is reasonable. Again, the results are virtually independent of the presence of either 1 or 150 mM SO_4^{2-}.

The inhibition of sulfate transport brought about by the combined actions of Cl^- and dipyridamole decreases with decreasing pH (Fig. 6). This effect can be accounted for almost entirely by assuming that only the deprotonated, uncharged form of dipyridamole combines with band 3 and produces inhibition while the mass law constants for Cl^- and dipyridamole binding (K_1 and K_8, respectively) are pH independent.

Assuming a pK for deprotonation of dipyridamole of 6.25 one can calculate that at pH 6.9 about 20% of the dipyridamole is protonated and hence ineffective. Using the data for K_8 in Table VI (1.47 μM at pH 6.9) one can calculate a value for the binding of uncharged dipyridamole of 1.18 μM. Inserting this latter value and the mass-law constant for Cl^- binding to the modifier site (K_1 = 24.2 mM, Table VI) into Eqn. A-3 and using the concentrations of deprotonated dipyridamole as calculated for each pH on the assumption of a pK of 6.25 one obtains the curves shown on Fig. 6. These predictions, based on independently obtained experimental data, represent the measurements reasonably well at least over the pH range 6.0–7.5.

(d) Models for the effects of dipyridamole on DBDS binding to band 3. (See Appendix B for quantitative treatment.)

The results presented in the previous sections suggest that the action of dipyridamole on stilbenedisulfonate binding to band 3 can be interpreted in terms of model II. This interpretation requires, however, assumptions about the location of the DBDS binding site. There exist several possibilities: DBDS (s) could bind to transfer site T, modifier site M or dipyridamole binding site P, or combinations thereof:

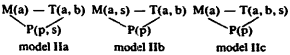

Our data are not reconcilable with model IIc which involves competition between stilbenedisulfonate and chloride for the transfer site. Such competition should lead to the disappearance of the effect of dipyridamole at high concentrations of either Cl^- or SO_4^{2-}, which is contrary to our observation (Figs. 1, 5). We shall confine, therefore, the discussion to models IIa and IIb.

Before discussing the effects of dipyridamole we shall consider DBDS binding in the absence and presence of either chloride or sulfate. According to Fröhlich [10] a related stilbenedisulfonate, DNDS, competes with Cl^- for binding to the transfer site. Our data show that the effect of Cl^- on DBDS binding is small (increasing the chloride concentration from 0 to 130 mM increases the $K_{1/2}$ value for DBDS binding from 0.68 μM to 1.1 μM) and that increasing the concentration of SO_4^{2-} which supposedly combines with the same transfer site as Cl^- causes, if anything, a slight reduction of $K_{1/2}$ from 0.68 μM to 0.5 μM. The effects of Cl^- on DNDS binding observed by Fröhlich are also small and not very different from our findings with DBDS. Hence, the small effects observed do not necessarily need to be interpreted as competition between stilbene and chloride at the transfer site and the absence of competition with another substrate, sulfate, argues against such interpretation.

Using the known values of $K_{1/2}$ for the binding of DBDS in the absence of dipyridamole, and of dipyridamole in the absence of DBDS, (both pertaining to the appropriate experimentally used chloride concentration), we find that the measured values agree reasonably well with the predictions of model IIa (Eqn. B-1) but

TABLE VII

Effect of dipyridamole on $K_{1/2}$ of DBDS binding to band 3. Comparison of experimental results with predictions of models IIa and IIb (evaluation of the data in Figs. 7a,b)

$K_{1/2}$ [a] and $K_{1/2}$ [b] were calculated by means of Eqns. B-1 and B-2, respectively. The following numerical values were inserted: K_1 = 24.2 mM, K_8 = 1.47 μM (average of the data in Table VI). Stilbene binding in the presence of 130 mM Cl^-, K_{16} = 1.42 μM; in the absence of both Cl^- and SO_4^{2-}, K_{14} = 0.68 μM; in the presence of 108 mM SO_4^{2-}, $K_{22} \approx K_{101}$ = 0.5 μM.

[Dipyridamole] (μM)	$K_{1/2}$ observed (mM)	$K_{1/2}$ [a] model IIa (mM)	$K_{1/2}$ [b] model IIb (mM)
0	1.1	1.2	4.3
32	26.8	23.5	83.9

* The slight systematic effects of SO_4^{2-} concentration on J_{rel} depicted in Fig. 5 are obscured by the scatter introduced by the estimate of numerical values for three independent constants (K_1, K_8, q_K) from a rather limited number of experimental data.

not with those of model IIb (Eqn. B-2). Thus these experiments suggest that dipyridamole and stilbenes compete for a common site which is neither identical to the transfer site nor to the chloride binding modifier site (Table VII).

This inference could be further tested by the numerical evaluation of experiments in which the release of DBDS by dipyridamole was measured as a function of Cl^- concentration. The increase of DBDS release with increasing $[Cl^-]$ could again be predicted by model IIa (Eqn. B-1) but not by model IIb (Eqn. B-2) (Fig. 8). It should be noted that in all predictions about the effect of dipyridamole and Cl^- on stilbene binding, values for K_1 and K_8 were used that had been derived from the independently executed studies of inhibition kinetics in which no stilbene had been used (Table VI).

Comments and Conclusions

Dipyridamole produces non-competitive inhibition of inorganic anion transport by combination with a modifier site that does not overlap with the transfer site. The binding site does seem to overlap, however, with the binding site for stilbenedisulfonates like DNDS (p. 199) or DBDS (p. 198). Many carefully executed and evaluated experiments suggest, that these latter agents compete with the substrate ions for the transfer site (reviewed in Ref. 9). This may mean that the binding sites for dipyridamole and stilbenes overlap only partially and that upon dipyridamole binding the substrate binding site retains its ability to bind the inorganic anions. Differences of the configuration of the band 3 molecule after the binding of stilbenedisulfonates and dipyridamole may also be expected on account of the fact that the stilbenes introduce two negative net charges while dipyridamole binding is associated with the binding of the negative net charge of one single chloride ion only.

Dipyridamole and stilbenedisulfonates are chemically totally unrelated (Fig. 11). However, molecular models of dipyridamole and representative stilbene inhibitors (e.g. DNDS, H_2DIDS) show remarkably similar geometry and dimensions, suggesting that they share the ability to enter the hydrophobic cleft that is supposed to accomodate the stilbenedisulfonates [9]. This would leave little room for significant differences of binding and hence for different effects on the accessibility of the transfer site for the substrate anions. Our results suggest, therefore, that it may be worthwhile to consider in future work whether or not stilbenedisulfonates compete in fact with the substrate. The absence of competition between SO_4^{2-} and DBDS reported here (p. 198) would support the need for such work.

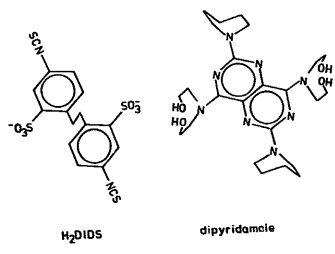

Fig. 11. Structural formulas of dipyridamole and H_2DIDS.

The quantitative evaluation of our data in terms of model IIa

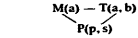

showed that the expected complexity of the interactions of two substrates and two inhibitors at three different sites is considerably reduced by the fact that the inhibition is non-competitive and almost entirely dominated by the allosteric interactions between the modifier site M and the common binding site P for stilbenes and dipyridamole. Thus, when the dissociation constants for the binding of chloride to M and for the binding of the dipyridamole and the stilbenedisulfonates to P are known, one could predict with reasonable accuracy the action of dipyridamole on both transport and stilbene binding as a function of the chloride concentration. The other allosteric interactions between the three sites seem to be of minor significance for the overall events.

Appendix A

Kinetics of anion transport inhibition by dipyridamole

Model I

M(a) — T(a, b, p)

Cl^- binding to the modifier site M enables dipyridamole (p) to combine with the transfer site T and to produce inhibition of transport by competition with Cl^- (a) and SO_4^{2-} (b).

Table VIII lists the various forms that the transport protein may assume in the presence or absence of a, b, p.

$\bar{E}$ = sum of all forms listed in Table VIII.

$$\bar{E} = \left(1 + \frac{a}{K_1} + \frac{a}{K_2} + \frac{a^2}{K_1 K_2} + \frac{a \cdot b}{K_1 K_6} + \frac{b}{K_5} + \frac{p}{K_{55}} + \frac{p \cdot a}{K_{66} K_1}\right) \frac{K_2}{b} [bE]$$

where a, b and p represent the concentrations of a, b and p, respectively.

TABLE VIII

T	M	Desig-nation	Definition of mass-law constants
–	–	E	
a	–	aE	[a]·[E] = K_2[aE]
b	–	bE	[b]·[E] = K_5[bE]
p	–	pE	[p]·[E] = K_{55}[pE]
–	a	Ea	[a]·[E] = K_1[Ea]
a	a	aEa	[a]·[Ea] = K_3[aEa]
b	a	bEa	[b]·[Ea] = K_6[bEa]
p	a	pEa	[p]·[Ea] = K_{66}[pEa]

Assuming $K_2 = K_3$, $K_5 = K_6$, $K_{55} = \infty$ (i.e., no dipyridamole binding to T without binding of a to M) one obtains

$$\bar{E} = \left[\left(1+\frac{a}{K_1}\right)\left(1+\frac{a}{K_2}+\frac{b}{K_5}\right)+\frac{p\cdot a}{K_{66}K_1}\right]\cdot\frac{K_5}{b}[\mathrm{bE}]$$

Sulfate flux $J_p = k_{12}[\mathrm{bE}] + k_{1122}[\mathrm{bEa}]$

$$J_p = \frac{b}{K_5}\cdot\frac{k_{12}+k_{1122}\dfrac{a}{K_1}}{\left(1+\dfrac{a}{K_1}\right)\left(1+\dfrac{a}{K_2}+\dfrac{b}{K_5}\right)+\dfrac{p\cdot a}{K_{66}K_1}}\cdot\bar{E}$$

Sulfate flux and dipyridamole concentration p relative to the flux at $p = 0$

$$J_{\mathrm{rel}} = \frac{J_p}{J_{p=0}} = \frac{\left(1+\dfrac{a}{K_1}\right)\left(1+\dfrac{a}{K_2}+\dfrac{b}{K_5}\right)}{\left(1+\dfrac{a}{K_1}\right)\left(1+\dfrac{a}{K_2}+\dfrac{b}{K_5}\right)+\dfrac{a\cdot p}{K_1K_{66}}} \qquad \text{(A-1)}$$

This equation implies:
(i) without Cl^- ($a = 0$) or dipyridamole ($p = 0$) no inhibition;
(ii) at $a \cdot p = \infty$, $J_{\mathrm{rel}} = 0$, i.e., maximal inhibition is complete inhibition. This consequence is contrary to experimental observation.

Model II

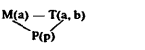

a = chloride, b = sulfate, p = dipyridamole, T = transfer site, M = Cl^- binding modifier site, P = dipyridamole binding modifier site.

Table IX lists the various forms that the transport protein may assume in the presence or absence of a, b, p.

$\bar{E}$ is the sum of all forms listed in Table IX.

$$E_1 = \mathrm{E} + \mathrm{Ea} + \mathrm{aEa} + \mathrm{aE} + \mathrm{bE} + \mathrm{bEa} = (K_5/b)\cdot X_1\cdot[\mathrm{bE}]$$

$$E_2 = \mathrm{Ep} + \mathrm{Eap} + \mathrm{aEap} + \mathrm{aEp} + \mathrm{bEp} + \mathrm{bEap} = (K_5/b)\,X_2\cdot p\cdot[\mathrm{bE}]$$

All symbols indicate concentrations. Where possible the square brackets were omitted for simplicity of representation. a, b and p represent the concentrations of a, b and p, respectively.

$$X_1 = 1 + \frac{a}{K_1} + \frac{a}{K_2} + \frac{a^2}{K_1K_3} + \frac{b}{K_5} + \frac{a\cdot b}{K_1K_6}$$

$$X_2 = \frac{1}{K_7} + \frac{a}{K_8K_1} + \frac{a}{K_{10}K_2} + \frac{a^2}{K_9K_1K_3} + \frac{b}{K_{11}K_5} + \frac{a\cdot b}{K_{12}K_1K_6}$$

Sulfate flux:

$$J_p = k_{12}[\mathrm{bE}] + k_{1122}[\mathrm{bEa}] + k_{1133}[\mathrm{bEap}] + k_{13}[\mathrm{bEp}]$$

$$J_p = \left(k_{12} + k_{1122}\frac{K_5a}{K_6K_1} + k_{1133}\frac{pK_5a}{K_{12}K_6K_1} + k_{13}[\mathrm{bEp}]\right)\cdot[\mathrm{bE}]$$

where

$$[\mathrm{bE}] = (b/K_5)\cdot\bar{E}/(X_1 + X_2p).$$

Assuming $k_{12} = k_{1122}$, $k_{13} = k_{1133}$ and defining $k_{1133}/k_{12} = q_K$ yields:

$$J_p = k_{12}[\mathrm{E}]\cdot\frac{b}{K_5}$$

$$\cdot\frac{1 + K_5a/K_6K_1 + [(q_Kp)/K_{12}]\cdot(K_{12}/K_{11} + K_5a/K_6K_1)}{X_1 + X_2\cdot p}$$

Sulfate flux at dipyridamole concentration p relative to the flux at $p = 0$:

$$J_{\mathrm{rel}} = \frac{J_p}{J_{p=0}} = \frac{\left[1 + \dfrac{K_5\cdot a}{K_6K_1} + q_K\dfrac{p}{K_{12}}\left(\dfrac{K_{12}}{K_{11}} + \dfrac{K_5\cdot a}{K_6K_1}\right)\right]\cdot X_1}{\left(1 + \dfrac{K_5\cdot a}{K_6K_1}\right)(X_1 + X_2p)} \qquad \text{(A-2)}$$

TABLE IX

T	M	P	Desig-nation	Definition of mass-law constants
–	–	–	E	
–	a	–	Ea	[E]·[a] = K_1[Ea]
a	–	–	aE	[E]·[a] = K_2[aE]
a	a	–	aEa	[Ea]·[a] = K_3[aEa]
b	–	–	bE	[E]·[b] = K_5[bE]
b	a	–	bEa	[Ea]·[b] = K_6[bEa]
–	–	p	Ep	[E]·[p] = K_7[Ep]
–	a	p	Eap	[Ea]·[p] = K_8[Eap]
a	a	p	aEap	[aEa]·[p] = K_9[aEap]
a	–	p	aEp	[aE]·[p] = K_{10}[aEp]
b	–	p	bEp	[bE]·[p] = K_{11}[bEp]
b	a	p	bEap	[bEa]·[p] = K_{12}[bEap]

This expression can be transformed into

$$J_{rel} = \frac{1 + \tau_1 a + \tau_2 a^2 + \tau_3 a^3}{1 + \tau_4 a + \tau_5 a^2 + \tau_6 a^3}$$

where the τ values represent coefficents that are functions of p, b and the various mass-law constants K, but not of a.

For the special case:
$K_2 = K_3$, $K_5 = K_6$, i.e., binding of Cl^- or SO_4^{2-}, respectively, to transfer site T is not affected by binding of Cl^- to modifier site M;
$K_8 = K_9 = K_{12}$, i.e., dipyridamole binding to modifier site P is only affected by Cl^- binding to modifier site M but not by Cl^- or SO_4^{2-} binding to transfer site T;
$K_7 = K_{10} = K_{11} = \infty$, i.e., no dipyridamole binding without Cl^- binding to modifier site M;
follows:

$$X_1 = \left(1 + \frac{a}{K_1}\right)\left(1 + \frac{a}{K_2} + \frac{b}{K_5}\right)$$

$$X_2 = \left(\frac{a}{K_8 K_1} + \frac{1}{K_7}\right)\left(1 + \frac{a}{K_2} + \frac{b}{K_5}\right)$$

and one obtains for J_{rel} an expression without quadratic or cubic terms

$$J_{rel} = \frac{J_p}{J_{p=0}} = \frac{1 + \alpha_2 a}{1 + \alpha_4 a} \qquad \text{(A-3)}$$

where

$$\alpha_2 = \frac{1}{K_1}\left(1 + q_K \frac{p}{K_8}\right) \text{ and } \alpha_4 = \frac{1}{K_1}\left(1 + \frac{p}{K_8}\right)$$

This equation implies:
(i) without Cl^- ($a = 0$) or dipyridamole ($p = 0$) no inhibition: $J_{rel} = 1.0$;
(ii) at high concentrations of Cl^- ($a = \infty$) the flux J_{rel} tends towards the asymptotic value α_2/α_4, which is a function of p and q_K, where the experiments show that $q_K \ll 1.0$.

For $J_{rel} = 0.5$ one obtains the half-inhibition constant $K_{1/2}$ for dipyridamole:

$$K_{1/2} = \frac{0.5 K_8}{0.5 - q_K} \cdot \left(\frac{K_1}{a} + 1\right) \qquad \text{(A-4)}$$

which yields for $q_K \ll 0.5$ (cf. Table VI):

$$K_{1/2} = K_8\left(\frac{K_1}{a} + 1\right) \qquad \text{(A-5)}$$

and for the limiting case $a \gg K_1$:

$$K_{1/2} = K_8$$

Appendix B

Effect of dipyridamole on stilbenedisulfonate binding

Within the frame of reference of model II there exist three possible sites for stilbene binding:

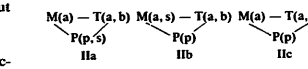

The symbols have the same meaning as in Appendix A. s refers to stilbenedisulfonates, like DNDS or DBDS.

Using these shorthand descriptions of the three possibilities for stilbene binding, it is easily possible to extend the derivations in Appendix A to include the various forms that arise as a consequence of stilbene binding, using the following definitions:

Model IIa

Competition between p and s for modifier site P.

$$[E] \cdot s = K_{14}[Es],\ [Ea] \cdot s = K_{16}[Eas],\ [aEa] \cdot s = K_{18}[aEas]$$

$$[aE] \cdot s = K_{20}[aEs],\ [bE] \cdot s = K_{22}[bEs],\ [bEa] \cdot s = K_{24}[bEas]$$

$$\bar{E} = E_1 + E_2 + E_3$$

where:

$$E_3 = [Es] + [Eas] + [aEas] + [aEs] + [bEs] + [bEas]$$

$$= (K_5/b) \cdot X_3 \cdot [bE]$$

with

$$X_3 = \frac{1}{K_{14}} + \frac{a}{K_1 K_{16}} + \frac{a^2}{K_1 K_3 K_{18}} + \frac{a}{K_2 K_{20}} + \frac{b}{K_{22} K_5} + \frac{a \cdot b}{K_1 K_6 K_{24}}$$

If $K_2 = K_3$, $K_5 = K_6$, $K_8 = K_9 = K_{12}$, $K_7 = K_{10} = K_{11} = \infty$, (i.e., the same assumptions as in Appendix A) and $K_{14} = K_{20} = K_{22}$, $K_{16} = K_{18} = K_{24}$ (i.e., the binding of s to modifier site P is affected by the absence or presence of bound Cl^- at modifier site M), then

$$X_3 = \frac{1}{K_{14}}\left(1 + \frac{K_{14} a}{K_{16} K_1}\right)\left(1 + \frac{a}{K_2} + \frac{b}{K_5}\right)$$

Using the pertinent expressions for E_1 and E_2 in Appendix A one obtains

$$E_3 = \frac{s}{s + K_{1/2}} \qquad \text{(B-1)}$$

where

$$K_{1/2} = K_{14} \frac{1 + \frac{a}{K_1}\left(1 + \frac{p}{K_8}\right)}{1 + \frac{K_{14} a}{K_{16} K_1}}$$

Model IIb

Effect of binding of p to modifier site P on competition of a and s for modifier site M.

$$[E]\cdot s = K_{101}[Es],\ [Es]\cdot a = K_{102}[aEs],\ [Es]\cdot b = K_{106}[bEs]$$

$$[Es]\cdot P = K_{108}[Esp],\ [aEs]\cdot p = K_{109}[aEsp],\ [bEs]\cdot p = K_{112}[bEsp]$$

$$\bar{E} = E_1 + E_2 + E_4$$

where

$$E_4 = [Es] + [aEs] + [bEs] + [Esp] + [aEsp] + [bEsp]$$

Experimentally we observe that dipyridamole binding removes the stilbenedisulfonate from band 3. Hence, $[Esp] = [aEsp] = [bEsp] = 0$. We may write, therefore,

$$E_4 = [Es] + [aEs] + [bEs] = (K_5/b)\cdot X_4\cdot[bE]$$

If $K_{102} = K_2$, $K_{106} = K_6 = K_5$, (i.e. stilbene binding to M has no effect on Cl^- or SO_4^{2-} binding to transfer site T) then:

$$X_4 = \frac{s}{K_{101}}\left(1 + \frac{a}{K_2} + \frac{b}{K_5}\right)$$

Using the appropriate expressions for E_1 and E_2 in Appendix A one obtains:

$$E_4 = \frac{s}{s + K_{1/2}} \qquad \text{(B-2)}$$

where

$$K_{1/2} = K_{101}\left[1 + \frac{a}{K_1}\left(1 + \frac{p}{K_8}\right)\right]$$

Model IIc

Effect of binding of a to M and of p to P on competition among a, b and s for the transfer site T.

$$K_{14} = K_{20} = K_{22},\ K_{16} = K_{18} = K_{24} \qquad \text{(see Model IIa)}$$

$$[E]\cdot s = K_{200}[sE],\ [Ea]\cdot s = K_{300}[sEa],\ [sEa]\cdot p = K_{90}[sEap],$$

$$[sE]\cdot p = K_{100}[sEp]$$

$$\bar{E} = E_1 + E_2 + E_5$$

where

$$E_5 = [sE] + [sEa] + [sEp] + [sEap] = (K_5/b)\cdot X_5\cdot[bE]$$

Assuming $K_2 = K_3$, $K_5 = K_6$, $K_8 = K_9 = K_{12}$, $K_7 = K_{10} = K_{11} = \infty$ and $K_{200} = K_{300}$ (i.e., stilbenedisulfonate binding independent of Cl^- binding to modifier site M), $K_{100} = \infty$ (i.e., no dipyridamole binding without Cl^- binding to M), one obtains

$$X_5 = \frac{1}{K_{200}}\left(1 + \frac{a}{K_1}\left[1 + \frac{p}{K_{90}}\right]\right)$$

$$E = \frac{s}{K_{1/2} + s} \qquad \text{(B-3)}$$

where

$$K_{1/2} = \frac{X_1 + X_2 p}{X_5} = \frac{1 + \frac{a}{K_1}\left(1 + \frac{p}{K_8}\right)\left(1 + \frac{a}{K_1} + \frac{b}{K_5}\right)}{\frac{s}{K_{200}}\left(1 + \frac{a}{K_1}\left[1 + \frac{p}{K_{90}}\right]\right)}$$

Acknowledgments

We thank Mrs. S. Lepke for the contribution of the binding studies, Mrs. E.-M. Gärtner for some of the kinetic experiments, and Dr. E. Grell for the provision of the equipment and his knowhow for the planning of the fluorescence experiments and the evaluation of the data. We are indebted to Prof. S. Svetina for helpful discussions about the theoretical aspects of this work, and to Dr. G. Fritzsch for reading the manuscript and many useful comments.

References

1 Goodman and Gilman's (1985) The Pharmacological Basis of Therapeutics, 7th Edn., McMillan, London.
2 Deuticke, B. (1970) Naturwissenschaften 57, 172.
3 Ku, C.P., Jennings, M.L. and Passow, H. (1979) Biochim. Biophys. Acta 553, 132–141.
Barzilay, M. and Cabantchik, Z.I. (1979) Membr. Biochem. 2, 297–322.
4 Cass, A. and Dalmark, M. (1973) Nature 244, 47–49.
5 Schwoch, G. and Passow, H. (1973) Mol. Cell. Biochem. 2, 197–218.
6 Rudloff, V., Lepke, S. and Passow, H. (1983) FEBS Lett. 163, 14–21.
7 Dix, J.A., Verkman, A.S., Solomon, A.K. and Cantley, L.C. (1979) Nature 282, 520–522.
8 Wood, P.G. and Passow, H. (1981) Techniques in Cellular Physiology, P 112, 1–43, Elsevier, North Holland, Amsterdam.
9 Passow, H. (1986) Rev. Physiol. Biochem. Pharmacol. 103, 61–203.
10 Fröhlich, O. (1982) J. Membr. Biol. 65, 111–123.
11 Passow, H., Fasold, H., Jennings, M.L. and Lepke, S. (1982) in Chloride Transport in Biological Membranes (Zadunaisky, J., ed.), pp. 1–31, Academic Press, New York.